IOP Conference Series: Materials Science and Engineering

PAPER • OPEN ACCESS

A New Approach to Debris Flow Study

To cite this article: Silvia Bosa *et al* 2019 *IOP Conf. Ser.: Mater. Sci. Eng.* **603** 032068

A New Approach to Debris Flow Study

Silvia Bosa [1], Marco Petti [1], Sara Pascolo [1], Cristiano Reolon [1]

[1] Università degli Studi di Udine, via del Cotonificio 114, 33100 Udine, Italy

silvia.bosa@uniud.it

Abstract. This work presents a first application of an open source SPH model (DualSPHysics) to study the dynamics of a debris flow, with reference to the dry debris flow of Alverà, close to Cortina d'Ampezzo (Belluno, Italy). In this part of the Dolomites, debris flows are usually formed by large boulders within the fluid matrix. The adopted Lagrangian approach has allowed to describe the relative motion of a boulder immersed in a fluid mixture. From the numerical results, it has been observed that the boulder travels a greater distance along the channels, when water drives it. On the other hand, without the water thrust, the same boulder would halt much earlier. Furthermore, in all the simulated cases, it has been observed that the boulder stops when a natural narrowing is encountered along the channel bed.

1. Introduction

The UNESCO World Heritage of the Dolomites represents a very important site for economic activities linked to tourism, especially in the summer and winter seasons, when tens of thousands of tourists populate small mountain villages [1]. Nevertheless, this territory is also very fragile and it presents several situations at risk of landslides and collapses [2] that in the past have triggered disastrous events, such as the case of Vajont dam [3]. The town of Cortina d'Ampezzo, in the heart of the Dolomites, is particularly exposed to debris flow risk, that threatens buildings, infrastructures and the population. This natural phenomenon can often travel great distances in a short time, reaching houses and streets with its great destructive power. The risk reduction of these events is made even more arduous by the difficulty that the engineers encounter in predicting when and where they can occur [4].

Debris flows are a mixture of water and sediments, that may contain large solid elements with a size comparable to the dimension of the flow depth. Nevertheless, they are usually studied as a continuum [5] with relevant bulk properties that may change in time and space. In this context, many different types of mass movements are regarded as debris flows [6]: debris torrents, debris floods, mudflows, mudslides, hyper-concentrated flows. The forces that support the largest stones and boulders during their movement are mainly related to the dispersive pressure resulting from collisions among the particles [7] and the plastic strength of the interstitial fluid when this is composed of a clay or mud slurry [8]. In this sense, the turbulence of the interstitial fluid would be too weak to support the largest particles [9].

The risk induced by a debris flow can be reduced with a correct modeling of the phenomenon and a consequent adequate territorial management [10].

An effective protection against these issues starts from the knowledge of these phenomena and an attempt to predict their effects [11]. For example, the forecast of the characteristics of a debris flow such as the propagation speed and the distances traveled is of great importance for the planning of the protective structures [12]. In this perspective, it is necessary to adequately represent the dynamics of a debris flow, through a numerical modeling, that allows to correctly interpret the physical phenomenon

[13]. Generally, the study of a debris flow is carried out following an Eulerian approach, i.e. in which the solid-liquid mixture is treated as a continuous [14].

Nevertheless, the presence of large boulders with a diameter which can reach and exceed 5 meters is typical in the Dolomites debris flows. The modeling of these boulders by means of a homogeneous mixture casting is not possible, because it would not pick up the relative motion of a solid element within the flow. Therefore, it is preferable to choose a Lagrangian approach to follow the movement of the boulders within a fluid matrix [15].

With this in mind, in this work a new approach is presented to study debris flows through a Smoothed-Particle Hydrodynamics (SPH) method, which is based on the Lagrangian description of the movement of a set of particles that discretize a continuous. SPH method was first developed to solve astrophysical problems in three-dimensional open space [16-17]. Recently, it has also been extended to a vast range of problems in fluid mechanics given the possibility to incorporate complex physics into its formulations [18-20]. SPH methods are an alternative to the more classic Eulerian methods that usually adopt bi-dimensional shallow water equations, and which can be generally applied in the same contexts. For example, the wave generated by the Vajont landslide, right in the territory of the Dolomites, has been studied both with an Eulerian approach and with the SPH method [21-23].

In the present paper, the open source SPH model DualSPHysics [24] has been applied to represent the phenomenon that affects Cortina d'Ampezzo (BL) known as the "debris flow of Alverà". As a first approach, the debris flow was modeled through water and boulders of considerable size, identifying important characteristics such as propagation speed and traveled distances, in order to correctly assess the risk and to propose adequate actions to mitigate it.

In section 2 the SPH model is described, some tests are presented in section 3 and finally the results of the Alverà debris flow simulation are reported in section 4.

2. SPH model

In SPH methods the state of a system is represented by a set of particles, which possess material properties and interact with each other within the range controlled by a *kernel function* (also called *weight function* or *smoothing function*), denoted by W [25]. The SPH method was originally developed for hydrodynamic problems in which the motion is described by means of partial differential equations of field variables such as density, velocity, energy and so on. Basically, two steps are needed to get a proper SPH formulation. The first step, called kernel approximation, consists in representing a generic vector function $\bar{\boldsymbol{f}}(\bar{\mathbf{x}})$ and its derivatives with an integral which is then discretized. The second step is defined as approximation of the particles, when the computational domain is discretized with a particle distribution that best represents the initial condition. The field variables associated with a particle are therefore obtained as a weighted sum of the values assumed by the variables corresponding to the closest particles, where the weights are provided by the kernel function (Figure 1).

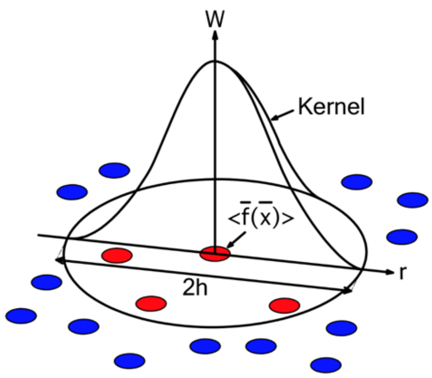

Figure 1. Schematic illustration of kernel function.

Different smoothing functions have been used in the SPH methods [26-27] and various requirements or properties for the smoothing functions have been discussed [28-30]. In the present paper, the open source SPH model DualSPHysics, developed by Domìnguez and coworkers, has been used [31]. DualSPHysics adopts one of the most frequently used smoothing function, that is the cubic B-spline function (Figure 1), which was originally proposed by Monaghan and Lattanzio [32]. The kernel (W) represents a weight through which a generic vector function $\bar{\boldsymbol{f}}(\bar{\mathbf{x}})$ can be expressed in an integral form, and hence the discrete form and relative derivatives can be obtained.
Using SPH approximation techniques, it is possible to derive several formulations for the equations governing the fluid motion. DualSPHysics adopts Navier-Stokes (N-S) equations in the formulation derived by [33-34]. In particular, the momentum equation can be written as:

$$\frac{D\bar{\mathbf{v}}_i^{\alpha}}{Dt} = -\sum_{j=1}^{N} m_j \left(\frac{P_i^{\alpha\beta}}{\rho_i^2} + \frac{P_j^{\alpha\beta}}{\rho_j^2} + \Pi_{ij}\right)\frac{dW_{ij}}{dx_i^{\beta}} + F_i^{\alpha} \tag{1}$$

where the superscripts α and β are used to denote the coordinate directions, the sum in the equations is taken over repeated indices, and the total time derivatives are taken in the moving Lagrangian frame. F^{α} (component of external force $\bar{\mathbf{F}}$ in α direction) is the external forces such as gravity. The spatial coordinates x^{β} and time t are the independent variables. The subscript i refers to the considered particle and the subscript j considers the neighboring particles. $\bar{\mathbf{v}}$ represents the velocity, m the mass, P the pressure, ρ the density, W the kernel. The viscous term Π can be written as:

$$\Pi_{ij} = \begin{cases} \dfrac{-\alpha\tilde{c}_{ij}\mu_{ij}}{\tilde{\rho}_{ij}} & \bar{\mathbf{v}}_{ij}\cdot\bar{\mathbf{x}}_{ij} < 0 \\ 0 & \bar{\mathbf{v}}_{ij}\cdot\bar{\mathbf{x}}_{ij} > 0 \end{cases} \tag{2}$$

where $\bar{\mathbf{v}}_{ij} = \bar{\mathbf{v}}_i - \bar{\mathbf{v}}_j$, $\bar{\mathbf{x}}_{ij} = \bar{\mathbf{x}}_i - \bar{\mathbf{x}}_j$, $\tilde{\rho}_{ij} = \frac{1}{2}(\rho_i + \rho_j)$ is the average density from the particles i and j, $\tilde{c}_{ij} = \frac{1}{2}(c_i + c_j)$ the average sound speed from the particles i e j, μ_{ij} is a parameter $\mu_{ij} = \frac{h\bar{\mathbf{v}}_{ij}\cdot\bar{\mathbf{x}}_{ij}}{(\bar{\mathbf{x}}_{ij}^2+\eta^2)}$ in which $\eta^2 = 0{,}01h^2$ while α is a calibration parameter depending on the material.
A key point of every model is the assignment of boundary conditions. In DualSPHysics kinematic boundary conditions, such as a rigid wall, are defined by dummy particles (Figure 2) [35].

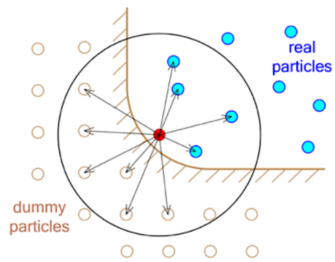

Figure 2. Schematic illustration of kinematic boundary condition.

Dynamic boundary conditions, such as the no-slip condition, are defined in a dissipative form through the Tait equation of state, which links the particle pressure to particle density [36]:

$$P = B\left[\left(\frac{\rho}{\rho_0}\right)^{\gamma} - 1\right] \tag{3}$$

Parameter B is a constant related to the modulus of elasticity of the fluid; $\rho_0 = 1000 \frac{kg}{m^3}$ is the reference density usually considered as the density of the fluid on the free surface, γ is the polytropic constant generally assumed between 1 and 7 (equal to 7 if the fluid is water). The term -1 in the square brackets guarantees zero pressure on the free surface.

In the SPH method, it is important to correctly establish the value of the VBF parameter, which represents the ratio between the α parameters of respectively bottom material and water. In all the performed simulations, the value of the VBF parameter was obtained through a correlation with the Gauckler-Strickler coefficient.

3. Test cases

Before proceeding with the case study of the debris flow of Alverà, some tests have been performed in order to validate the model by comparison with an analytical solution. In the following, two tests are shown: the first regards a sphere that rolls on an inclined plane and the second one refers to a uniform flow in a channel. These tests have been chosen since they represent important aspects of a debris flow.

3.1 Sphere that rolls on an inclined plane

In this paragraph the test of a sphere, that rolls without crawling on a 4-m long and 15.596° inclined plane on the horizontal, is described [37]. The sphere starts from a standstill and travels a height difference *h*. In absence of friction, it is possible to evaluate the final speed of the sphere, applying the mechanical energy conservation. This test could be representative of a boulder, that rolls down the mountain in a debris flow, neglecting the presence of the fluid fraction and hence it can be regarded as a preliminary analysis to apply the model to a real event.

Since the domain of the problem is small, it is convenient to discretize both sphere and plane with small particles, i.e. assigning a small distance between the particles *dp*, so that the objects belonging to the domain are represented with adequate precision. In the present test a value of *dp* = 0.01 m has been chosen; it follows that the sphere has been discretized through 1956 particles while the inclined plane has been represented with 494 particles.

The test is schematically summarized in Figure 3, where *v* is the final velocity of the sphere, *g* the gravity acceleration and *h* the height.

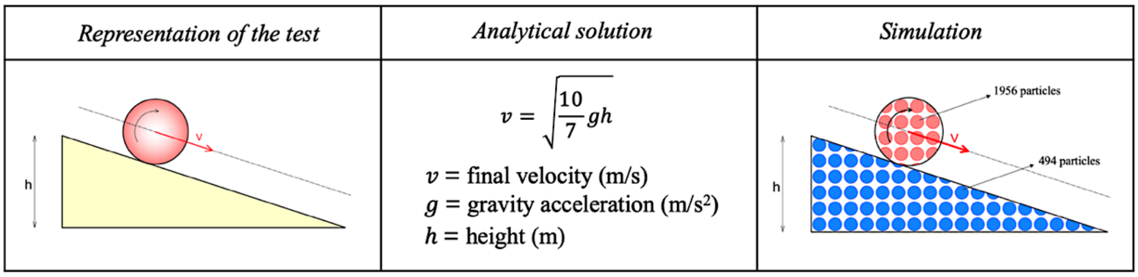

Figure 3. Schematic illustration of the simulation of the sphere that rolls on an inclined plane.

The test has been carried out for different values of the plane height *h* and Table 1 shows for each simulation the comparison between analytical and numerical velocities, with the relative error.

Table 1. Comparison between analytical and numerical solutions for different test configurations.

h (m)	$v_{analytical}$ (m/s)	$v_{numerical}$ (m/s)	Error (%)
1.0	3.743	3.718	0.67
1.5	4.584	4.562	0.48
2.0	5.294	5.272	0.42

It can be observed that the test provides satisfactory results, the relative error being always less than 1%.

3.2 Uniform flow in a channel

In a uniform flow both the intrinsic properties of the fluid and the characteristics of the motion are independent of space and time; in particular, in the case of a current of incompressible fluid both the average current velocity U and the wet cross section Ω remain constant along the flow direction.

A good representation of a uniform flow requires a sufficiently long channel, so that the flow reaches a steady state in time and space. In the hypothesis of an infinitely large riverbed, it is preferable to consider a bi-dimensional vertical domain (2DV) rather than a tridimensional one; this helps in reducing the particles number, maintaining a good accuracy in discretizing the problem. The fluid is described by 16212 particles and the bottom is represented by 4472 particles.

The test is schematically summarized in Figure 4, where U is the average flow velocity, k_s the Gauckler-Strickler factor, h the height and i_f the bed slope.

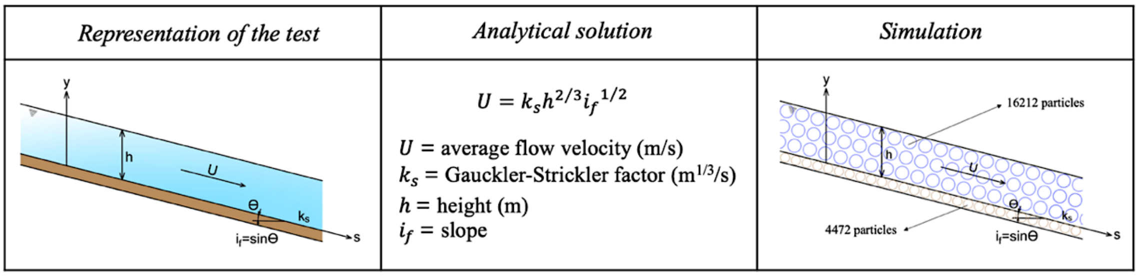

Figure 4. Schematic illustration of the simulation of the uniform flow in a channel.

Different configurations of bed slope, water depth, and VBF parameter, which is linked to k_s, have been performed. Table 2 shows the comparison between analytical and numerical velocities, and the relative error.

Table 2. Comparison between the analytical and numerical solutions for different test configurations.

k_s (m$^{1/3}$/s)	i_f (%)	h (m)	$U_{analytical}$ (m/s)	$U_{simulation}$ (m/s)	Error (%)
10	0.1	0.62	0.230	0.230	0.00
22.73	0.1	0.98	0.712	0.703	1.26
25	0.1	1.00	0.791	0.807	1.98
27.78	0.1	1.08	0.925	0.931	0.65
28	0.1	1.10	0.944	0.961	1.80
29.41	0.1	1.18	1.038	1.053	1.41
35.7	0.1	1.30	1.345	1.323	1.64
40	0.1	1.32	1.521	1.528	0.46

The error, contained within 2%, is considered acceptable for engineering applications.

4. Debris flow of Alverà

The domain adopted for the Alverà's debris flow simulations extends from Mount Cristallo to the village of Alverà - Cortina d'Ampezzo (Figure 5), and it has been built by means several orthophotos and the Regional Technical Charter, while the bottom elevation has been assigned through the lidar surveys available from the Civil Engineering Department of Belluno.

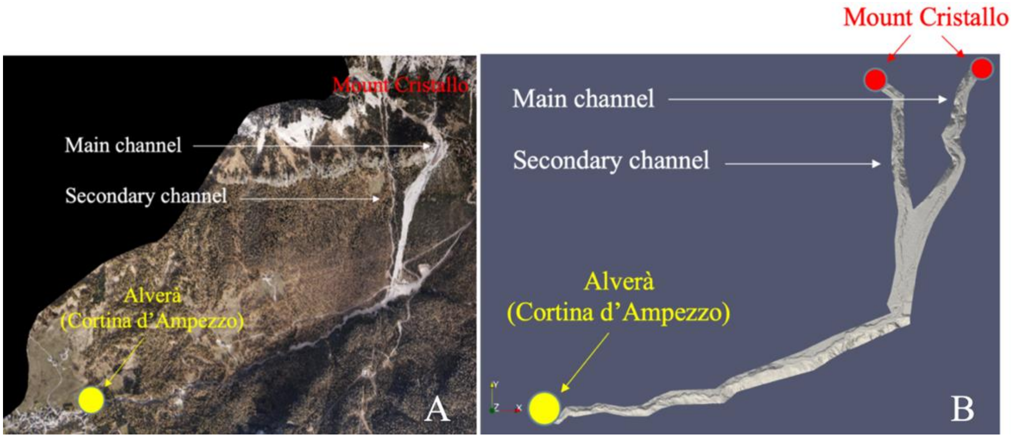

Figure 5. (a) Orthophoto of the domain area. (b) Alverà's debris flow simulation domain.

It has been decided to proceed by intermediate steps to study such a complex phenomenon. First, the debris flow of Alverà has been assimilated to a dry debris flow, that is a mixture of water and boulders; moreover, in this work just one boulder has been introduced. In all cases, the same bottom roughness has been assigned with $k_s = 22{,}73$ m$^{1/3}$/s.

Before simulating the mixture water – boulder, two separate simulations have been carried out: the former has considered only water (Figure 6a) and the latter only the boulder (Figure 6b).

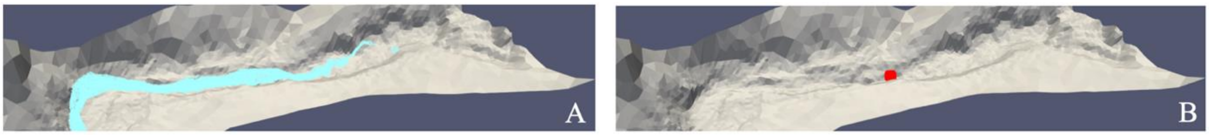

Figure 6. (a) Simulation of water only. (b) Simulation of boulder alone.

4.1 Simulation of water only

In this simulation the distance between particles has been assumed equal to 0.4 m, so that the channels have been represented with 2522476 particles and the water body with 34148 particles. As the initial condition, a water volume at rest of 6000 m^3 has been positioned in the upper part of the main channel; this is comparable with the volume recorded in some previous events in the same area. The flow reaches the village of Alverà after 16 minutes.

Figure 7a-c shows the results respectively after 20, 200 and 1000 s. It can be observed that in the initial stretch of the channel, where the slope is greater, the water velocity is high, while after the confluence it reduces as the slope decreases.

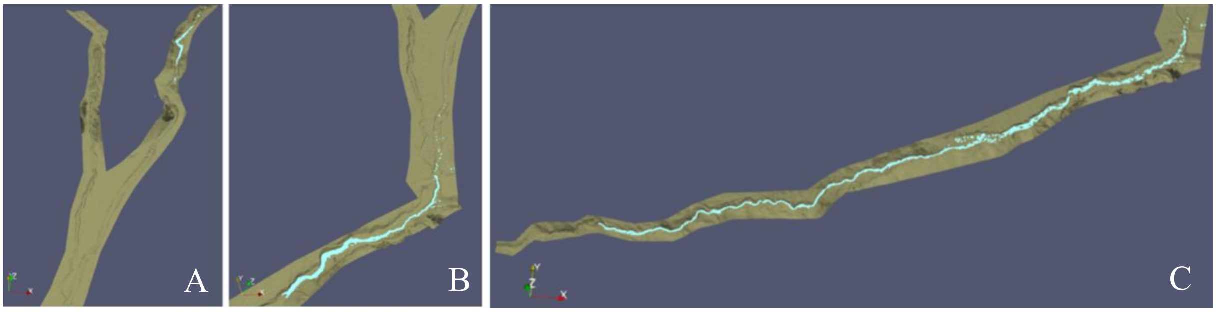

Figure 7. Results after: (a) 20 s; (b) 200 s; (c) 1000 s.

IOP Conf. Series: Materials Science and Engineering **603** (2019) 032068 doi:10.1088/1757-899X/603/3/032068

4.2 Simulation of boulder alone

Also in this test a distance between particles of 0.4 m has been imposed, that is the channels have been represented with 2522476 particles and the boulder with 374 particles. Based on the surveys carried out post-event 4-5 August 2017, several simulations have been carried out according to different boulder dimensions, as it has been schematized by a sphere with a variable radius between 1.2 and 2.4 meters. In the present paper, the results of the simulation with a 2.0 m radius boulder are presented.

As initial conditions, it has been assumed that the boulder detached from the Mount Cristallo and run along the main channel. Figure 8a-c shows the results respectively after 5, 20 and 50 s. It can be observed that after about 150 meters (Figure 8c) the boulder stops due to a natural narrowing of the channel bed (Figure 9).

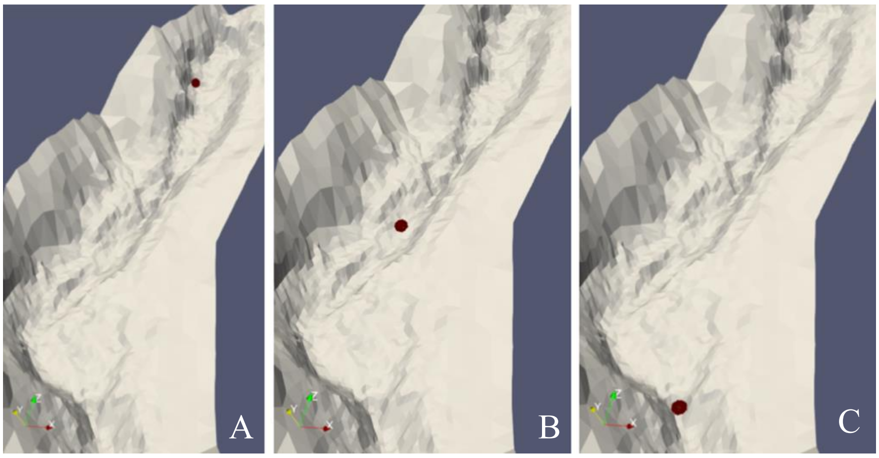

Figure 8. Results after: (a) 5 s; (b) 20 s; (c) 50 s.

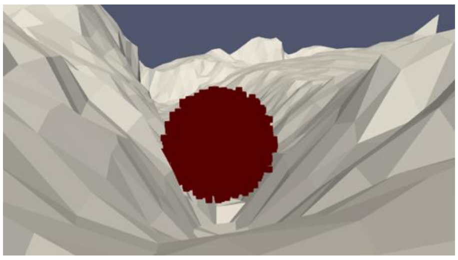

Figure 9. Natural narrowing present in the channel bed.

In Figure 10 the speed of all boulder solid particles can be observed after 45 s.

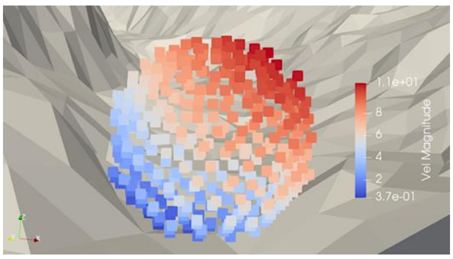

Figure 10. Speed of the solid particles that make up the boulder after a 45 s.

IOP Conf. Series: Materials Science and Engineering **603** (2019) 032068 doi:10.1088/1757-899X/603/3/032068

4.3 Simulation with water and boulder

The final simulation consists in the simultaneous presence of water and the boulder in the main channel. Figure 11a-c shows the results after respectively 5, 20 and 40 s. Here, the position of the boulder in the previous simulation without water at the same time steps is also depicted (in yellow), to allow a comparison between the two situations.

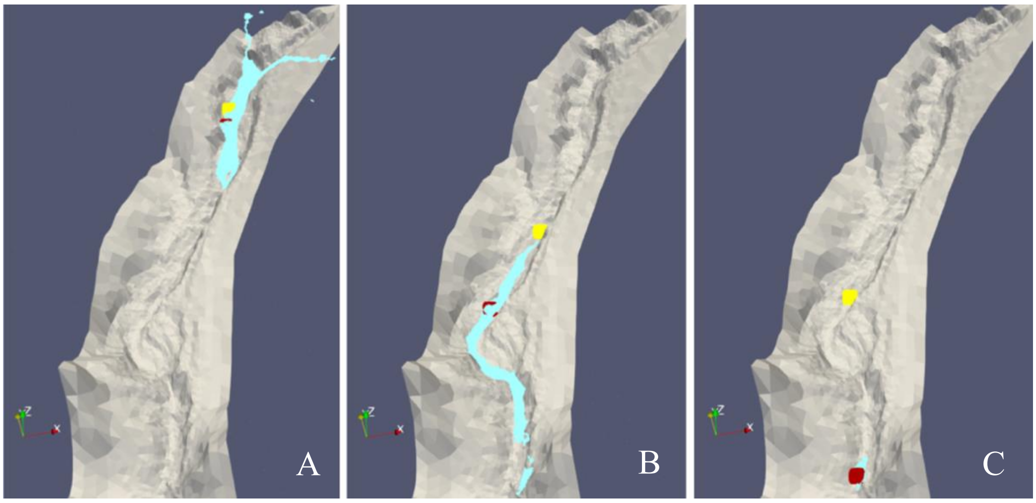

Figure 11. Results after: (a) 5 s; (b) 20 s; (c) 40 s. In red the boulder with water, in yellow the boulder alone.

It can be observed that the boulder travels about 350 meters, more than twice the distance of the case without water. Therefore, it can be concluded that the water thrust has a significant influence on the problem, allowing the boulder to overcome some small natural narrowing present along the channel.

5. Conclusions

In the present paper, the DualSPHysics model, based on a Lagrangian SPH method, has been applied to study the dynamics of a debris flow in a real domain. In the authors' knowledge this is the first time that this technique has been used to simulate this kind of phenomena.

As a first approach, some simple tests have been carried out to validate the model and a simplified simulation of the debris flow of Alverà has been conducted, considering a dry debris flow, consisting of water and a single boulder.

Despite the simplifications, interesting results and features that would not have been visible with a traditional Eulerian approach, have been obtained. In particular, the simulations have shown that the thrust of water greatly affects the problem, since the boulder stops earlier when it is no longer dragged by the flow. Moreover, in all the examined cases, the boulder stops when it finds natural narrowing in the riverbed along its path. This result suggests possible interventions along the riverbed, such as the construction of artificial bottlenecks in appropriate sections, with the aim to mitigate the risk that the boulders reach the downstream inhabited areas. Nevertheless, this issue should be studied more in depth to develop optimal defense strategies.

Future developments of this study should be addressed to the study of the behavior of several boulders immersed in a muddy mixture. A drawback of SPH methods is the high number of particles that are required for an accurate discretization of the domain. This problem makes these techniques still difficult to apply to large domains such as those described for example in [38-39]. A possible further idea to overcome this issue could be the coupling of the SPH model for the boulders with an Eulerian model for the fluid flow, as it has already done in the maritime field, where spectral model has been coupled to morphodynamic model [40-42].

References

[1] M. Panizza, "Outstanding Intrinsic and Extrinsic Values of the Geological Heritage of the Dolomites (Italy)," *Geoheritage*, vol. 10, pp. 607-612, 2018.

[2] R. Casale, C. Margottini, "Natural Disasters and Sustainable Development", *Springer-Verlag Berlin Heidelberg*, ISSN 1431-6250, 2004.

[3] C. Datei, "Vajont. La storia idraulica", Cortina, Padova, 2003 (in italian).

[4] M. B. Zolin, P. Ferretti, K. Némedi, "Multi-criteria decision approach and sustainable territorial subsystems: An Italian rural and mountain area case study," *Land Use Policy*, vol. 69, pp. 598-607, 2017.

[5] C. Ancey, "Plasticity and geophysical flows: a review," *Journal of Non-Newtonian Fluid Mechanics*, vol. 142, pp. 4–35, 2007.

[6] R. M. Iverson, "The physics of debris flows," *Reviews of Geophysics*, vol. 35, pp. 245–296, 1997.

[7] R. A. Bagnold, "Experiments on a gravity-free dispersion of large solid spheres in a Newtonian fluid under shear," *Proceedings of the Royal Society of London*, vol. 225, pp. 49–63, 1954.

[8] P. Coussot, C. Ancey, "Rheophysical classification of concentrated suspension and granular pastes," *Physical Review*, vol. 59, pp. 4445–4457, 1999.

[9] T. Takahashi, "Mechanical characteristics of debris flow," *Journal of Hydraulic Division*, vol. 104, pp. 1153–1169, 1978.

[10] H. X. Lan, L. P. Li, Y. S. Zhang, X. Gao, H. J. Liu, "Potential hazard analysis and risk assessment of debrisflow by fuzzy modeling," *Natural Hazards*, vol. 64, pp. 273-282, 2012.

[11] L. Canelli, A. Ferrero, M. Migliazza, A. Segalini, "Debris flow risk mitigation by the means of rigid and flexible barriers - experimental tests and impact analysis," *Natural Hazards And Earth System Sciences*, vol. 12, pp. 1693-1699, 2012.

[12] S. Lambert, F. Bourrier, D. Toe, "Improving three-dimensional rockfall trajectory simulation codes for assessing the efficiency of protective embankments," *International Journal of Rock Mechanics and Mining Sciences*, vol. 60, pp. 26-36, 2013.

[13] M. Pastor, A. Yague, M. M. Stickle, D. Manzanal, P. Mira, "A two-phase SPH model for debris flow propagation," *International Journal for Numerical and Analytical Methods in Geomechanics*, vol. 42, pp. 418-448, 2018.

[14] K. Ota, T. Sato, H. Nakagawa, "Quantification of spatial lag effect on sediment transport around a hydraulic structure using Eulerian-Lagrangian model," *Advances in Water Resources*, 2017.

[15] M. Cremonesi, A. Frangi, U. Perego, "A Lagrangian finite element approach for the analysis of fluid-structure interaction problems," *International Journal for Numerical Methods in Engineering*, vol. 84, pp. 610-630, 2010.

[16] R. A. Gingold, and J. J. Monaghan, "Smoothed particle hydrodynamics theory and application to non-spherical stars," *Monthly Notices of The Royal Astronomical Society*, vol. 181, pp. 375–389, 1977.

[17] L. B. Lucy, "A numerical approach to the testing of the fission hypothesis," *Astronomical Journal*, vol. 82, pp. 1013–1024, 1977.

[18] G. R. Liu, and M. B. Liu, "Smoothed particle hydrodynamics: A meshfree particle method." *World Scientific Publishing Company*, Singapore, 2003.

[19] P. W. Cleary, M. Prakash, J. Ha, N. Stokes, and C. Scott, "Smooth particle hydrodynamics: Status and future potential," *Progress In Computational Fluid Dynamics*, vol. 7, pp. 70–90, 2007.

[20] J. J. Monaghan, "Smoothed particle hydrodynamics and its diverse applications," *Annual Review Of Fluid Mechanics*, vol. 44, pp. 323–346, 2012.

[21] S. Bosa, M. Petti, "Shallow water numerical model of the wave generated by the Vajont landslide", *Environmental Modelling and Software*, vol. 26, pp. 406-418, 2011.

[22] S. Bosa, M. Petti, "A Numerical Model of the Wave that Overtopped the Vajont Dam in 1963", *Water Resources Management*, vol. 27, pp. 1763-1779, 2013.

[23] R. Vacondio, P. Mignosa, S. Pagani, "3D SPH numerical simulation of the wave generated by the Vajont rockslide", *Advances in Water Resources*, vol. 59, pp. 146-156, 2013.

[24] A. J. C. Crespo, M. Gòmez-Gesteira, and R. A. Dalrymple, “Modeling dam break behavior over a wet bed by an SPH technique,” *Journal of Waterway, Port, Coastal and Ocean Engineering*, vol. 134, pp. 313-320, 2008.
[25] D. A. Fulk, and D. W. Quinn, “An analysis of 1-D smoothed particle hydrodynamics kernels,” *Journal of Computational Physics*, vol. 126, pp. 165–180, 1996.
[26] M. Omang, S. Borve, and J. Trulsen, “Alternative kernel functions for smoothed particle hydrodynamics in cylindrical symmetry,” *Shock Waves*, vol. 14, pp. 293–298, 2005.
[27] J. W. Swegle, D. L. Hicks, and S. W. Attaway, “Smoothed particle hydrodynamics stability analysis,” *Journal of Computational Physics*, vol. 116, pp. 123–134, 1995.
[28] J. P. Morris, “A study of the stability properties of smooth particle hydrodynamics,” *Publications of the Astronomical Society Of Australia*, vol. 13, pp. 97–102, 1996.
[29] G. R. Johnson, and S. R. Beissel, “Normalized smoothing functions for SPH impact computations,” *International Journal for Numerical Methods in Engineering*, vol. 39, pp. 2725–2741, 1996.
[30] X. F. Yang, S. L. Peng, and M. B. Liu, “A new kernel function for SPH with applications to free surface flows,” *Applied Mathematical Modelling*, vol. 38, pp. 3822–3813, 2014.
[31] A. J. C. Crespo, M. Gòmez-Gesteira, and R.A. Dalrymple, “3D SPH Simulation of large waves mitigation with a dike,” *Journal of Hydraulic Research*, vol. 45, pp. 631–642, 2007.
[32] J. J. Monaghan, J. J. and J. C. Lattanzio, “A refined particle method for astrophysical problems,” *Astronomy and Astrophysics*, vol. 149, pp. 135–143, 1985.
[33] P. W. Randles and L. D. Libersky, “Smoothed particle hydrodynamics: Some recent improvements and applications,” *Computer Methods in Applied Mechanics and Engineering*, vol. 139, pp. 375–408, 1996.
[34] J. S. Chen, C. Pan, C. T. Wu, and W. K. Liu, “Reproducing kernel particle methods for large deformation analysis of nonlinear structures,” *Computer Methods in Applied Mechanics and Engineering*, vol. 139, pp. 195–227, 1996.
[35] J. M. Domìnguez, A. J. C. Crespo, M. Gòmez-Gesteira, J. C. Marongiu, “Neighbour lists in smoothed particle hydrodynamics,” *International Journal for Numerical Methods in Fluids*, vol. 67, pp. 2026-2042, 2011.
[36] S. Tait, M. Muthusamy, A. Schellart, M. N. A. Beg, R. F. Carvalho, J. L. M. P. de Lima, “Improving understanding of the underlying physical process of sediment wash-off from urban road surfaces,” *Journal of Hydrology*, vol. 557, pp. 426-433, 2018.
[37] D. Halliday, J. Walker, and R. Resnick, “Fundamentals of Physics,” *John Wiley and Sons Inc*, USA, 2013.
[38] M. Petti, S. Bosa, S. Pascolo, “Lagoon Sediment Dynamics: A Coupled Model to Study a Medium-Term Silting of Tidal Channels”, *Water*, 10, 569, 2018.
[39] S. Bosa, M. Petti, S. Pascolo, “Numerical Modelling of Cohesive Bank Migration”, *Water*, 10, 961, 2018.
[40] S. Pascolo, M. Petti, S. Bosa, “Wave–Current Interaction: A 2DH Model for Turbulent Jet and Bottom-Friction Dissipation”, *Water*, 10, 392, 2018.
[41] S. Pascolo, M. Petti, S. Bosa, “On the Wave Bottom Shear Stress in Shallow Depths: The Role of Wave Period and Bed Roughness”, *Water*, 10, 1348, 2018.
[42] M. Petti, S. Pascolo, S. Bosa, G. Fontolan, A. Bezzi. "Tidal flats morphodynamics: a new conceptual model to predict the evolution over medium-long period". *Water* **2019**, *11*(6), 1176; https://doi.org/10.3390/w11061176..